textbfit cmbxti10 textbfss cmssbx10 mathbfit cmbxti10 mathbfss cmssbx10

2000

Mon. Not. R. Astron. Soc. **000**, 2–11 (2000)

Scaling of N-body calculations

H. Baumgardt
Department of Mathematics and Statistics, University of Edinburgh, King's Buildings, Edinburgh EH9 3JZ

Accepted . Received ; in original form

ABSTRACT
We report results of collisional N-body simulations aimed to study the N-dependance of the dynamical evolution of star clusters. Our clusters consist of equal-mass stars and are in virial equilibrium. Clusters moving in external tidal fields and clusters limited by a cut-off radius are simulated. Our main focus is to study the dependence of the lifetimes of the clusters on the number of cluster stars and the chosen escape condition. We find that star clusters in external tidal fields exhibit a scaling problem in the sense that their lifetimes do not scale with the relaxation time. Isolated clusters show a similar problem if stars are removed only after their distance to the cluster centre exceeds a certain cut-off radius. If stars are removed immediately after their energy exceeds the energy necessary for escape, the scaling problem disappears.
We show that some stars which gain the energy necessary for escape are scattered to lower energies before they can leave the cluster. Since the efficiency of this process decreases with increasing particle number, it causes the lifetimes not to scale with the relaxation time. Analytic formulae are derived for the scaling of the lifetimes in the different cases.

Key words: celestial mechanics, stellar dynamics - globular clusters: general.

1 INTRODUCTION

The aim of the present paper is to study the dependence of the lifetimes of star clusters on the number of cluster stars and the chosen escape condition. It is important to understand this dependence, since at present it is impossible to perform a fully collisional simulation of globular clusters with realistic particle numbers. Hence, one has to scale the results of simulations with smaller particle numbers to the globular cluster regime (as for example in Wielen 1988), or adjust the parameters of other methods for star cluster evolution, for example Fokker-Planck calculations, such that they match the results of the largest feasible N-body calculations, like in Takahashi & Portegies Zwart (2000). In both cases it is important that the scaling of the lifetimes with the particle number is understood.

The theory for the dependence of the lifetime on the number of cluster stars was developed by Ambartsumian (1938) and Spitzer (1940). It is based on the assumption that the majority of more distant encounters between cluster stars is responsible for the mass-loss of the cluster. Distant encounters tend to set up a Maxwellian velocity distribution at each point inside the cluster. Such a distribution has non-zero density for every energy, so there are always stars which have velocities higher than the escape velocity of the cluster. These stars will escape, causing a steady mass-loss of the cluster.

Distant encounters lead to energy changes on the relaxation timescale (Chandrasekhar 1942, Spitzer 1987 eq. 2-62):

$$t_r = \frac{0.065\ v_m^3}{n\ m^2\ G^2\ ln\,\Lambda}\ , \tag{1}$$

where n is the density of cluster stars, m the mean mass of a star, v_m the average velocity of the stars, G the constant of gravitation and Λ is proportional to the number of cluster stars. During each relaxation time a constant fraction of cluster stars is scattered to energies above the escape velocity, so the lifetimes of star clusters should be multiples of their relaxation times.

There are however effects not accounted for by this theory. Hénon (1960) for example studied isolated clusters and showed that in this case the energy changes due to distant encounters are unimportant for escape, and instead most stars escape due to single close encounters with other cluster stars. In this and a later paper (Hénon 1969), he showed that this will lead to a scaling of the lifetime proportional to the number of cluster stars times the crossing time of the cluster.

Another complication was first pointed out by Chandrasekhar (1942) and studied in detail by King (1959). Since stars with energies high enough for escape need time to leave the cluster, some of them may be scattered back to lower energies and become bound again. This reduces the number of stars escaping from a cluster, thereby increasing its lifetime. If the escape time is constant, this effect will be more

important for low-N clusters, since their relaxation times are shorter and a higher fraction of potential escapers is retained. Backscattering therefore causes a deviation from a scaling with the relaxation time.

Further complications arise if external forces act upon a star cluster. Clusters moving on elliptic orbits through their parent galaxies for example are subject to tidal heating, which acts on the orbital timescale and is independent of the cluster's relaxation time. Since the changing tidal field removes stars, the lifetime of a cluster does not depend on the relaxation time alone. Similar problems exist if star clusters have to pass through galactic discs (Ostriker, Spitzer & Chevalier 1972, Weinberg 1994ab) or the mass-loss of the cluster stars is taken into account (Chernoff & Weinberg 1990, Fukushige & Heggie 1995).

Even for the simpler problem of a circular orbit with no individual mass loss of the cluster stars, the lifetime does not necessarily scale with the relaxation time. This was demonstrated by the Collaborative Experiment (Heggie et al. 1998), where multi-mass clusters moving in circular orbits around a point-mass galaxy were simulated. Clusters containing between 1024 and 65536 stars were studied and it was found that the lifetimes of the clusters increased more slowly than their relaxation times. Since there is some uncertainty in the correct definition of the relaxation time for a multi-mass cluster, it was however not clear if the observed discrepancy could not be removed by a different definition of the relaxation time.

It is the aim of the present paper to give a better understanding of the dependence of the lifetime on the number of cluster stars. We begin by studying simpler clusters with a tidal cut-off and use the results obtained there to understand the behaviour of clusters in a steady tidal field.

2 DESCRIPTION OF THE RUNS

The calculations were performed with the collisional Aarseth N-body code NBODY6++ (Makino & Aarseth 1992, Aarseth 1999). This code uses an Hermite integration scheme with block time-steps and Ahmad-Cohen neighbour scheme for the integration. It has recently been parallelised (Spurzem 1999, Spurzem & Baumgardt 2000) by means of MPI-routines to increase its peak performance.

All our clusters consist of equal-mass stars and their density distributions are given by $W_0 = 3.0$ King profiles. The tidal radii of the King models are adjusted such that they are equal to the cut-off radii for the isolated clusters, and are equal to the tidal radii given by the galactic tidal fields in the models with a full tide.

Clusters containing between 128 and 16384 stars were simulated. Small N clusters were simulated more than once in order to reduce the statistical noise. The evolution of small N clusters was followed on a Pentium III PC, while clusters with $N = 16384$ stars were simulated on a CRAY T3E parallel computer using 8 or 16 processors. With 8 processors, it took about 550 CPU-hours to follow the evolution of a King $W_0 = 3.0$ cluster with 16384 stars until complete dissolution.

Three different types of runs were performed: First we studied isolated clusters and removed stars if their energies were large enough so that they could reach the tidal radius. In the second case we also studied isolated clusters, but removed stars if their distance to the cluster centre exceeded the tidal radius. Simulations of this kind are often used to study tidally limited clusters. We finally studied clusters moving on circular orbits around point-mass galaxies with a proper tidal field.

Table 1. Details of the performed N-body runs.

Energy Cutoff

N	N_{Sim}	T_{Half}	σ_{T_H}
128	128	53.5	1.0
256	96	85.6	1.0
512	32	141.6	1.3
1024	8	239.5	4.8
2048	4	423.6	6.4
4096	2	739.6	16.0
8192	2	1320.9	33.0
16384	1	2371.5	

Radial Cutoff

N	N_{Sim}	T_{Half}	σ_{T_H}
128	96	107.3	2.3
256	64	155.8	1.9
512	32	234.6	2.5
1024	16	363.0	3.2
2048	8	585.0	9.1
4096	4	996.8	10.8
8192	2	1704.5	7.3
16384	1	2894.5	

Full tidal field

N	N_{Sim}	T_{Half}	σ_{T_H}
128	128	89.4	1.2
256	64	126.7	1.6
512	32	182.6	3.8
1024	16	258.5	4.2
2048	8	372.9	6.6
4096	4	558.1	5.2
8192	2	840.9	1.1
16384	1	1176.8	

Table 1 gives an overview of the simulations performed. The columns contain from left to right the number of cluster stars N, the number N_{Sim} of simulations performed, the mean time required to lose half the mass and an error estimate for the half-mass time. The error estimate was derived by calculating the standard deviation of the individual runs around the mean half-mass time and dividing it by the square root of N_{Sim}. We use the half-mass time to study the scaling in order to avoid very low N effects. These might play a role for the smallest clusters at the end of their lifetime.

All times are given in N-body units, where the total mass and energy of a cluster are given by $M = 1$ and $E_C = -0.25$ initially, and the constant of gravitation G is equal to 1. We will use these units throughout the paper.

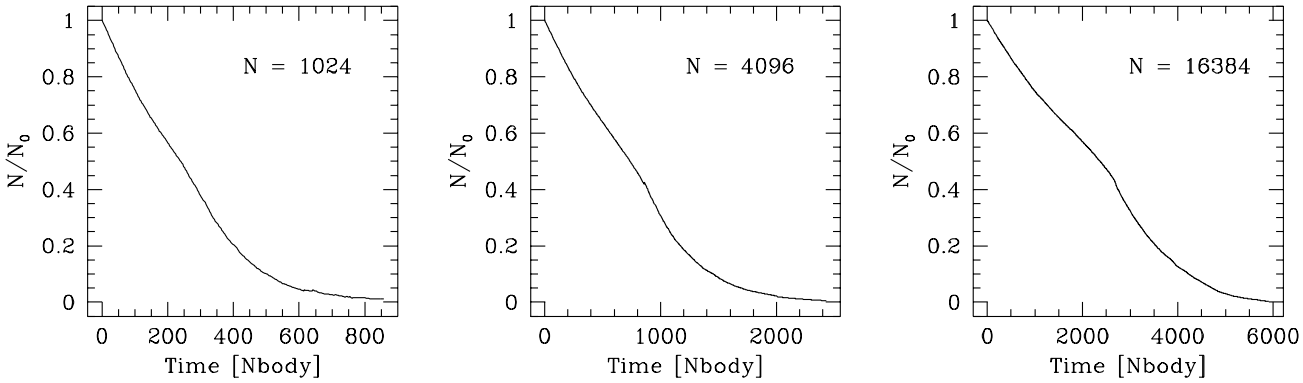

Figure 1. Evolution of the fraction of bound stars as a function of N-body time for three energy cut-off clusters. Shown is the mean of all clusters containing 1024, 4096 and 16384 stars initially.

3 RESULTS

3.1 Energy cut-off models

In the energy cut-off case, we immediately remove stars once their energies become high enough so that they can reach the tidal radius r_t of the cluster. The maximum distance r_m that a star at a distance r from the cluster centre can reach, provided it does not experience any encounters with other cluster stars, is given by the following equation:

$$\phi(r_m) + \frac{1}{2}v_\perp^2(\frac{r}{r_m})^2 = \phi(r) + \frac{1}{2}(v_{||}^2 + v_\perp^2) \qquad (2)$$

where $\phi(r)$ is the potential at position r and $v_{||}$ and $v_\perp$ denote the velocity components parallel and perpendicular to the direction from the star's position to the cluster centre. Note that the second term on the left hand side has to be added due to the conservation of angular momentum. Since we remove stars if they can reach the tidal radius, the energy E_{Crit} necessary for escape is given by:

$$E_{Crit} = -\frac{M_C}{r_t} + 0.5 \cdot \frac{\vec{L}^2}{r_t^2} \ , \qquad (3)$$

where L denotes the angular momentum of the star with respect to the cluster centre and M_C is the present mass of all stars still bound to the cluster. We check the energy of each star while it is advanced in the regular integrational part of NBODY6++ and all stars with energies larger than their critical energy E_{Crit} are immediately removed. The tidal radius r_t is kept fixed during the calculation in order to minimize the influence of drift in energy space of individual cluster stars due to the mass-loss of the cluster. Our model resembles many Fokker-Planck or gaseous models for star cluster evolution, in which the tidal field is treated as an energy boundary, and stars beyond this boundary are immediately removed.

Figure 1 shows the evolution of the number of bound stars (for the energy cut-off models equal to all stars still in the simulation) for three energy cut-off clusters. The number of bound stars decreases almost linearly until 90% of them are lost. There is a slight increase in the mass-loss rate at around core-collapse (which occurs after 60% of the stars are lost, see Fig. 3). The slow-down of the mass-loss at the end of the simulations can be explained by the constant tidal radius of our clusters. Due to this the outer lagrangian radii also remain nearly constant, so the crossing time becomes very large at the end. Hence the clusters evolve only slowly. It is therefore better to use the half-mass times of the clusters to study the scaling. This also avoids effects due to the core-collapse of the clusters.

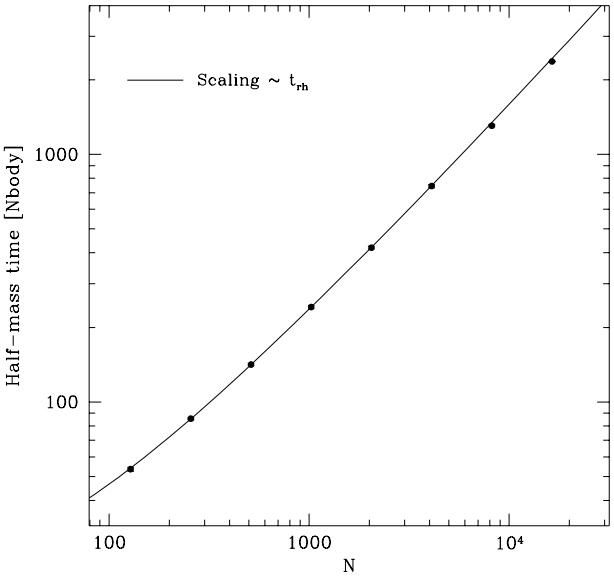

Figure 2. Mean half-mass times as a function of the number of cluster stars for the energy cut-off clusters. The solid line shows a theoretical scaling with the relaxation time, fitted to the mean half-mass time for $N = 1024$. It provides an excellent fit to the half-mass times of the N-body runs (filled circles).

Figure 2 shows the half-mass times as a function of the number of cluster stars. The solid line shows a scaling proportional to the half-mass relaxation time, fitted to the results of the $N = 1024$ runs. The half-mass relaxation time was taken from Spitzer (1987), eq. 2-63

$$t_{rh} = 0.138\frac{\sqrt{N}\ r_h^{3/2}}{\sqrt{m}\ \sqrt{G}\ \ln(\gamma N)} \ , \qquad (4)$$

with the value of the Coulomb logarithm taken to be $\gamma = 0.11$. Such a value was obtained by Giersz & Heggie (1994) by a comparison of the evolution of single-mass clusters containing $N = 500$ and $N = 2000$ stars respectively. As can be seen, a scaling proportional to the half-mass relaxation time

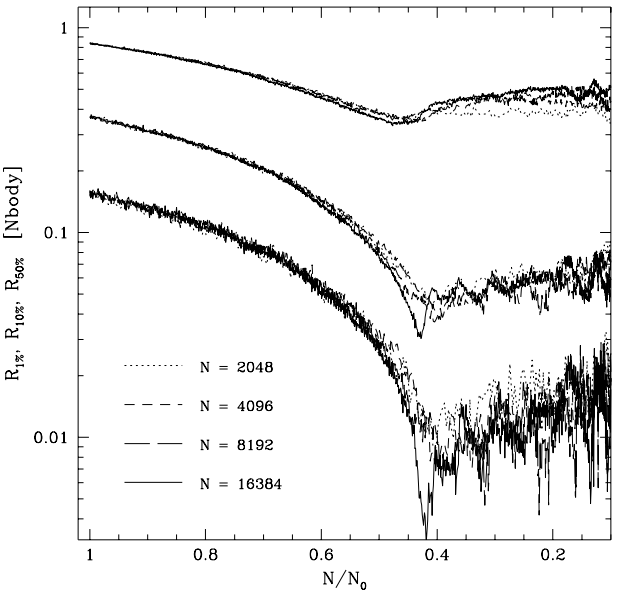

Figure 3. Evolution of the lagrangian radii containing 1, 10 and 50 % of all stars, as a function of the number of stars for clusters with $2048 \leq N \leq 16384$ initially. The graphs for different N lie on top of each other, showing that both quantities change on the same timescale.

provides an excellent fit to the N-body results. Following an idea of Toshio Fukushige, we can also check the scaling of the lifetimes without adopting a specific formula for the relaxation time. Figure 3 shows the evolution of the lagrangian radii as a function of the number of stars still bound to the clusters for clusters containing between $2048 < N < 16384$ stars initially. The change in the lagrangian radii is due to the core-collapse, which is generally believed to happen on the relaxation timescale since it is driven by two-body relaxation. If the mass-loss of the clusters is also happening on the relaxation timescale, one expects the graphs for different N to lie on top of each other. Otherwise differences in the scaling laws of both quantities should create different curves for different N. As can be seen in Fig. 3, the curves lie on top of each other, at least in the pre-collapse phase. The differences between the clusters around and after core-collapse are due to the different degrees of central concentration the clusters reach for different initial particle number and are not in contradiction with the pre-collapse evolution.

Combining the results of Figures 2 and 3, we conclude that the dissolution of the energy cut-off clusters happens on the relaxation timescale, and that eq. 4 with $\gamma = 0.11$ provides a good description for the relaxation time of single-mass clusters. We will therefore use it to study the scaling of the other models.

3.2 Radial cut-off models

The radial cut-off case differs from the models in the previous section only by the escape condition. Here, we remove stars after they have crossed the tidal radius r_t of the cluster, i.e. their distance to the cluster centre exceeds r_t. As in the energy cut-off case, the tidal radius is kept fixed during the integration.

Figure 4 shows the half-mass times of the radial cut-off clusters. The solid line shows a scaling with the relaxation time, fitted to the result of the largest run. There is a clear deviation from such a scaling. The half-mass times are sufficiently close to the expected curve only for the two largest models. Otherwise, they increase more slowly with N than the relaxation time.

In the radial cut-off models stars need time to travel from the place where they are scattered above the critical energy to the tidal radius of the cluster. While they move outward, potential escapers may be scattered back to lower energies and become bound again. This decreases the number of stars escaping from a cluster within a certain interval of time. To study the influence of backscattering, we divide the stars into three categories (bound stars with $E < E_{Crit}$, potential escapers with energies $E > E_{Crit}$, and escaped stars) and consider the processes shown in Figure 5: Stars are scattered into and out of the potential escaper regime on relaxation timescales and leave the clusters within one escape time. All three processes can be expected to be in equilibrium with each other, since the escape times are much shorter than the lifetimes of the clusters (see Table 2). We therefore obtain for N_{PE}:

$$\frac{dN_{PE}}{dt} = k_1 \frac{1}{t_{rh}} N_{Bound} - k_2 \frac{1}{t_{rh}} N_{PE} - \frac{1}{t_e} N_{PE} = 0 \qquad (5)$$

with the solution

$$N_{PE} = N_{Bound} \, \frac{k_1 t_e}{t_{rh} + k_2 t_e} \quad . \qquad (6)$$

Here N_{Bound} is the number of all stars with energies $E < E_{Crit}$ and k_1 and k_2 are constants which reflect the efficiencies for scattering stars above and below the critical energy. If the cluster mass decreases linearly with time, the lifetimes of the clusters (or in our case the half-mass times) can be estimated by dividing the number of all stars N_{Star} in the cluster by the number of stars escaping from the cluster within a given time interval. Hence

$$\begin{aligned} T_{Half} &= \frac{\frac{1}{2} N_{Star}}{\frac{1}{t_e} N_{PE}} \qquad (7) \\ &= \frac{1}{2k_1}(t_{rh} + (k_1 + k_2) t_e) \quad . \end{aligned}$$

This solution has two regimes. If $t_{rh} \gg (k_1 + k_2) t_e$, backscattering is unimportant since the timescale for it is much larger than the escape time. Hence, all stars scattered above the critical energy will escape, and the lifetime scales with the relaxation time. For smaller t_{rh}, backscattering leads to an increase of the lifetimes.

In order to fit our results, we have to determine the unknown quantities k_1, k_2 and t_e. The escape time can be measured in the simulations: For each escaping star we take the difference between the time it leaves the cluster and its last upward crossing of the critical energy E_{Crit}. This is done until the half-mass time is reached for a particular simulation and the mean over all simulations is taken. Table 2 gives the mean escape times determined that way. t_e increases slightly with N since potential escapers in high-N clusters acquire less energy before they leave the cluster due to the longer relaxation time. It therefore takes more time

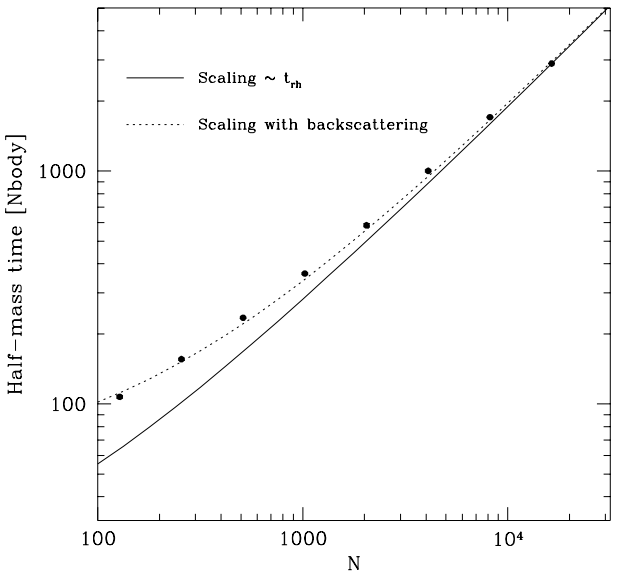

Figure 4. Mean half-mass times as a function of the number of cluster stars for the radial cut-off models. The solid line shows a scaling with the relaxation time fitted to the result of the largest run. There is a clear deviation from such a scaling. The dashed line shows the fit obtained by taking the influence of backscattering into account.

until they reach the tidal radius. In addition, the fraction of stars that escape due to large-angle encounters, which have large velocities and correspondingly small escape times, may drop with increasing N.

The constants k_1 and k_2 are best determined from a fit to the data. We find that $k_1 = 0.053$ and $k_2 = 1.01$ give the best fit. Figure 4 compares the predicted lifetimes with the N-body data for this choice of constants. There is good agreement between both, so a model with backscattering explains the N-dependence of the lifetimes.

The value required for k_1 means that high-N clusters lose a fraction $k_1 = 5.3{\cdot}10^{-2}$ of their mass during each relaxation time. This is only slightly higher then the value found by Spitzer (1987, eq. 3-27) $\xi_e = 4.5 \cdot 10^{-2}$ for the evolution of Hénon's self-similar model. It is also close to the values found by Johnstone (1993) from Fokker-Planck simulations of single-mass clusters surrounded by a tidal cut-off. Since he did not study King models with a central concentration of $W_0 = 3.0$, no direct comparison is possible, but judging from his results for $W_0 = 2.0$ and $W_0 = 4.0$, it seems that our mass-loss rate is again slightly larger. The reason may be that the Fokker-Planck approach neglects close encounters, which may be important in the cores of the clusters and contribute to the mass-loss.

The value for k_2 is rather high, since it implies that the process of backscattering is some 20 times more effective than the scattering of stars above the critical energy. It can be explained by the fact that stars are drifting only slowly through energy space, so a typical potential escaper has an energy only slightly above the critical energy. It is therefore easily scattered back to lower energies and becomes bound again, whereas it is much harder to scatter a bound star to energies above E_{Crit}.

Table 2. Mean escape times t_e and potential escaper fraction F_{PE} for the radial cut-off models. Shown is the mean over all simulations calculated up to the half-mass time.

N	t_e	$< F_{PE} >$ [%]
128	4.71	4.41
256	4.76	2.97
512	4.99	2.00
1024	5.23	1.29
2048	5.34	0.82
4096	5.55	0.49
8192	5.95	0.29
16384	6.43	0.14

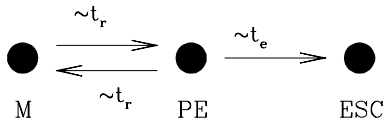

Figure 5. Model for the evolution of the radial cut-off clusters. Bound members (M) are scattered above the critical energy required for escape and become potential escapers (PE). Potential escapers are either scattered back before they can leave the cluster and become bound members again, or escape.

We finally compare the number of potential escapers in the N-body runs with our prediction. Table 2 lists the mean fraction of potential escapers, defined as $F_{PE} = \frac{N_{PE}}{N_{Star}}$, calculated from the beginning up to the half-mass times of the clusters. It is compared with eq. 6, with the relaxation time calculated at the point when the clusters have lost 25 % of their stars:

$$< F_{PE} > = < \frac{N_{PE}}{N_{Star}} > \approx \frac{k_1 t_e}{(k_1 + k_2) t_e + t_{rh(0.75N_0)}} \quad . \quad (8)$$

Figure 6 compares the number of potential escapers with the predicted fraction. They both decrease with increasing N_0 due to the increase in the relaxation times and the predicted fraction gives a very good fit to the N-body results.

We conclude that the lifetimes of the radial cut-off models are influenced by backscattering. This process increases the lifetimes of low N-clusters. We expect that backscattering becomes unimportant for large enough N, since the relaxation time increases until all stars scattered above the critical energy will escape. Similar results were also found by King (1959). The main difference between his results and our work is that due to the small excess energies of potential escapers, backscattering is more important for radial cut-off clusters than estimated by him.

3.3 Clusters in a steady tidal field

We finally discuss the evolution of clusters moving in circular orbits around point-mass galaxies. In these models, the full tidal field is taken into account and stars are removed if their distance to the cluster centre exceeds twice the tidal radius. We note that the removal of stars has no influence on the scaling since it is made at a radius where nearly all stars are already unbound to the clusters.

In a constant tidal field, the tidal radius r_t and the

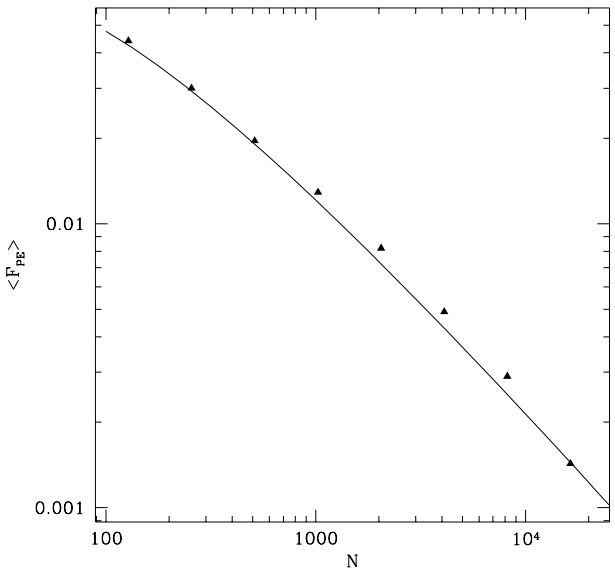

Figure 6. Mean potential escaper fraction as a function of the number of cluster stars. Triangles show the N-body results. The solid line shows the behaviour predicted by our model for backscattering.

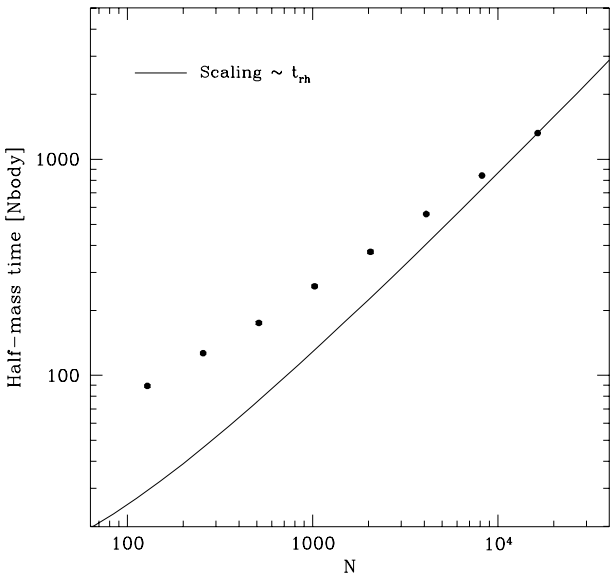

Figure 7. Same as Figure 2, but now for clusters in an external tidal field. There is a clear deviation from the expected scaling with the relaxation time. This deviation remains up to the highest simulated N. Compared to the highest run, the mean half-mass time of the $N = 128$ runs is a factor of 3 larger than expected.

critical energy required for escape are given by

$$r_t = \sqrt[3]{\frac{M_C}{3M_G}}\, R_G \tag{9}$$

$$E_{Crit} = -\frac{3}{2}\frac{M_C}{r_t}\ , \tag{10}$$

where R_G is the radius of the cluster orbit and M_G the mass of the galaxy. Since the critical energy gives only a necessary but not a sufficient criterion for escape, some stars can remain trapped inside the potential well even if their energies exceed E_{Crit}. For the other stars with $E > E_{Crit}$, the problem of their escape time was studied by Fukushige & Heggie (2000). They found that the time required for escape from a fixed potential is mainly a function of the excess energy $\Delta E = (E - E_{Crit})$ and drops approximately with this energy difference to the second power:

$$t_e \propto \left(\frac{E_{Crit}}{E - E_{Crit}}\right)^2\ . \tag{11}$$

This dependence arises since stars with energies slightly above the critical one can escape only through small apertures around the lagrangian points L_1 and L_2, which lie along the line connecting the cluster centre and the galaxy. These apertures become smaller and smaller as E approaches E_{Crit}. Hence stars have to pass through the cluster an increasing number of times before they find a hole in the potential well. The mean time required for escape is therefore much higher than in the radial cut-off case and backscattering of potential escapers should happen more often. In addition, potential escapers will also drift to higher energies because the cluster loses mass while they are still trapped inside the potential well of the cluster. This effect will certainly influence the number of potential escapers and shorten the lifetimes of the clusters. However, since it is happening on the dissolution timescale, it does not influence the scaling law.

Figure 7 shows the half-mass times as a function of the initial number of cluster stars. Compared to the radial cut-off clusters the discrepancy between a scaling with the relaxation time and the N-body results is larger and there is no sign that this discrepancy vanishes for higher particle numbers. One reason for the larger discrepancy between theory and N-body results is certainly the longer time that is required for escape in a tidal field. Figure 8 shows the evolution of the lagrangian radii as a function of the number of bound stars. The curves for different N do not lie on top of each other, instead core-collapse happens later for clusters with higher initial particle numbers. This means that the timescale for mass-loss differs from the timescale for core collapse, in agreement with Fig. 7. Summarising, Figs. 7 and 8 indicate that the lifetime does not scale with the relaxation time.

In order to understand the results of the N-body runs, we will neglect the fact that there are stars with $E > E_{Crit}$ that can never escape, and also the energy change of the stars due to the mass-loss of the cluster. We will also neglect dynamical friction, its influence will be discussed later. We take the energy dependence of the escape times into account, since the mean energy of potential escapers will change as a function of the number of cluster stars. Our model is comparatively simple, but should give an approximation to the processes happening in the N-body simulations.

We split the potential escaper regime into different energy bins E with particle numbers $N(E)$ (see Fig. 9). Utilising the expression for the escape times found by Fukushige & Heggie (eq. 11 of our paper), we obtain for the change of $N(E)$ with time:

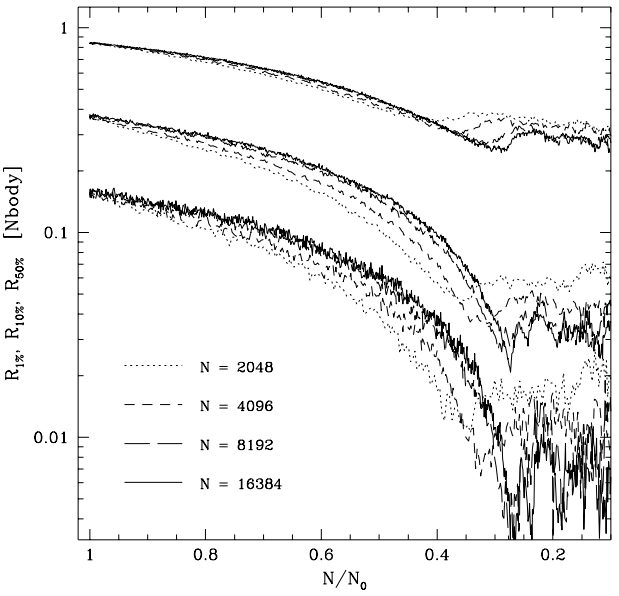

Figure 8. Same as Figure 3, but now for clusters in an external tidal field. The curves for different N do not lie on top of each other, instead core-collapse happens later for clusters with higher initial particle numbers. This confirms that the mass-loss is not happening on the relaxation timescale, in agreement with Figure 7.

$$\frac{dN(\hat{E})}{dt} = \frac{k_1}{t_{rh}} \frac{d^2N(\hat{E})}{d\hat{E}^2} - \hat{E}^2 \, \frac{N(\hat{E})}{t_{esc}} \tag{12}$$

Here the variable $\hat{E} = (E - E_{Crit})/E_{Crit}$ was introduced and t_{esc} is the time required for escape at energy $\hat{E} = 1$. Requiring equilibrium $dN(\hat{E})/dt = 0$ gives the following solution for $N(\hat{E})$:

$$N(\hat{E}) \propto \sqrt{\hat{E}} \, K_{\frac{1}{4}} \left(\frac{1}{2} \sqrt{t_{rh}/(k_1 \, t_{esc})} \hat{E}^2 \right) \tag{13}$$

with $K_{1/4}$ being a modified Bessel-function. Escape takes infinitely long for a star with zero excess energy, so the number of stars at $\hat{E} = 0$ is solely determined by the scattering of stars into the potential escaper regime and the backscattering of potential escapers, and should be proportional to the number N_{Star} of cluster stars:

$$N(\hat{E}) \propto N_{Star} \left(\frac{t_{rh}}{t_{esc}} \right)^{1/8} \sqrt{\hat{E}} \, K_{\frac{1}{4}} \left(\frac{1}{2} \sqrt{t_{rh}/(k_1 t_{esc})} \hat{E}^2 \right) \tag{14}$$

The mass-loss rate is given by

$$\begin{aligned} \dot{N}_{Esc} &= \frac{1}{t_{esc}} \int \hat{E}^2 \, N(\hat{E}) \, d\hat{E} \qquad (15) \\ &\propto N_{Star} \; t_{rh}^{-3/4} \; t_{esc}^{-1/4} \end{aligned}$$

and dividing the number of bound stars by $\dot{N}_{Esc}$ gives the following relation for the life time t_h:

$$t_h \propto t_{rh}^{3/4} \, t_{esc}^{1/4} \tag{16}$$

Hence, although the energy changes inside the cluster are assumed to happen on the relaxation time scale, we obtain the rather surprising result that the dissolution time scales with the relaxation time to the power of 3/4.

Figure 10 compares the $t_{rh}^{3/4}$ scaling with the N-body results. The agreement is good, the half-mass times in the N-body models increase only slightly slower with N than predicted. The reason for the small discrepancy may be that our clusters don't start with a potential escaper distribution that is in equilibrium. Our clusters start with primordial escapers since they are set up such that no star crosses the tidal radius only if the clusters are isolated. Since the tidal field adds a force which alters the potential energy of the cluster stars, some stars will initially have energies $E > E_{Crit}$. Their number and energy distribution will certainly not be the equilibrium one, so the initial phases until an equilibrium distribution is reached will show a different scaling. This may explain the slight differences.

Figure 11 shows the evolution of the potential escaper fraction with time. All clusters contain 15 % potential escapers initially due to the set-up. The slight increase of F_{PE} in the low-N clusters probably indicates the phase where the clusters evolve towards equilibrium. After equilibrium is

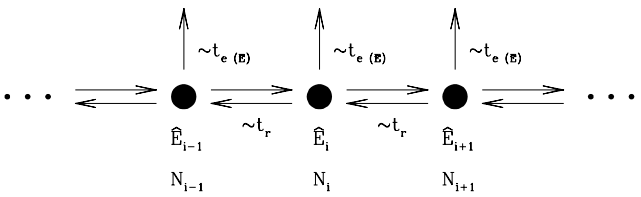

Figure 9. Model for the evolution of clusters in a steady tidal field. The potential escaper regime is split into different energies $\hat{E}$. Stars change their energies on the relaxation timescale and leave the cluster during the escape time t_e. The escape time drops with the energy difference $\hat{E} = (E - E_{Crit})/E_{Crit}$ to the second power $t_e \propto \hat{E}^{-2}$.

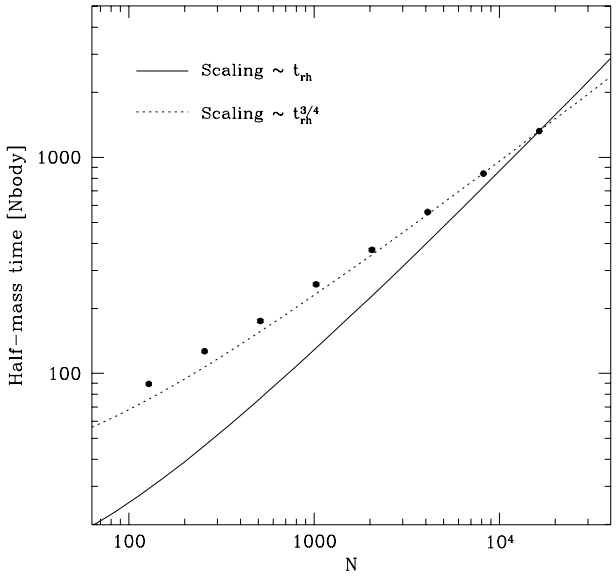

Figure 10. Comparison of the predicted $t_{rh}^{3/4}$ scaling with the N-body data for clusters in a tidal field. The theoretical curves are adjusted such to match the result of the highest run. A scaling proportional to $t_{rh}^{3/4}$ gives a good fit to the results of the N-body runs and is predicted by our theory.

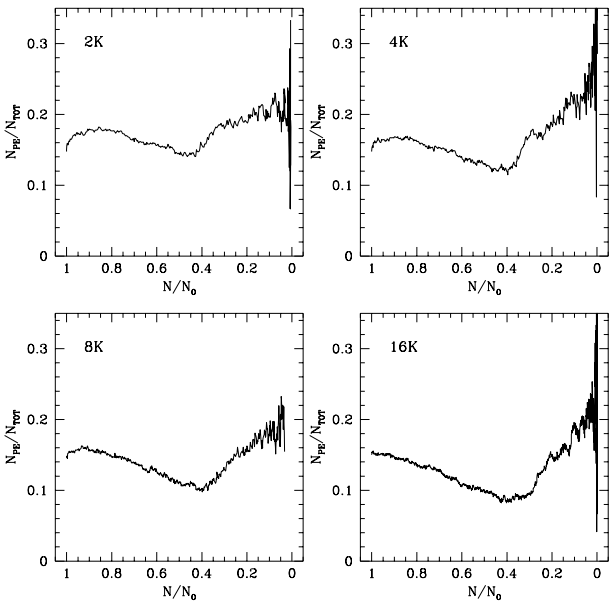

Figure 11. Potential escaper fraction for clusters in a tidal field as a function of the fraction of stars still bound to the clusters. The fraction drops until core-collapse and rises afterwards due to the increase of potential escapers from the core.

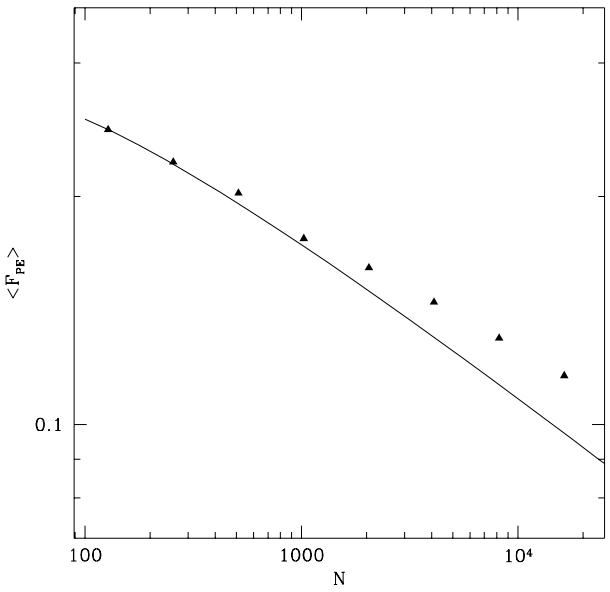

Figure 12. Mean potential escaper fraction as a function of the number of cluster stars. The solid line shows our prediction fitted to the results of the smallest runs. It provides a good fit only for $N \leq 1024$. Afterwards it drops too quickly, one reason being that bound members with $E > E_{Crit}$ were not taken into account.

reached, which happens at about $N/N_0 = 0.9$, the fraction of potential escapers drops until core-collapse. Core-collapse then causes a sharp increase in the fraction of potential escapers, and all models end up with a potential escaper fraction of about 20 %.

If we integrate the solution for $N(\hat{E})$ over all energies, our theory gives the following result for the dependance of the potential escaper fraction on the initial number of cluster stars:

$$F_{PE} = \frac{N_{PE}}{N_{Star}} = \frac{1}{N_{Star}} \int N(\hat{E}) d\hat{E} \propto t_{rh}^{-1/4} \quad (17)$$

Figure 12 compares the prediction with the mean escaper fraction of the N-body runs. To avoid effects due to the initial evolution, the mean fraction in the N-body runs was calculated between the time the clusters lost 10 % of their mass and the half-mass time. Both fractions decrease and we obtain a fit to the N-body results for clusters with $N \leq 1024$. Later the potential escaper fraction drops less quickly in the N-body results than in our theory. Part of this discrepancy is certainly due to bound members that have $E > E_{Crit}$ and that were neglected in our theory. The slow decrease means that even in clusters with particle numbers as high as globular clusters, several percent of the stars will have energies above the critical one.

Our results for the scaling of the lifetimes do not change if we add an energy drift term due to the mass-loss of the clusters to the right side of eq. 12. This might be expected, since the drift in energies is happening on the mass-loss timescale itself. If we add a term which is due to dynamical friction, eq. 12 becomes

$$\frac{dN(\hat{E})}{dt} = \frac{k_1}{t_{rh}} \frac{d^2 N(\hat{E})}{d\hat{E}^2} + \frac{k_2}{t_{rh}} \frac{dN(\hat{E})}{d\hat{E}} - \hat{E}^2 \frac{N(\hat{E})}{t_{esc}} \quad . \quad (18)$$

The corresponding solution for $N(\hat{E})$ are Whittaker functions. Numerical exploitation of the solution shows that if dynamical friction tends to slow down potential escapers, i.e. $k_2 > 0$, the scaling becomes flatter than in the case without friction. The change in the scaling vanishes for large N, in which case the dissolution times always scale proportional to $t_{rh}^{0.75}$.

The results presented so far were obtained for single-mass clusters. Figure 13 compares the predicted scaling with the half-mass times of multi-mass clusters. The data was taken from runs made by Sverre Aarseth and Douglas Heggie for the Collaborative Experiment. Their clusters had a Salpeter like mass-function, but are otherwise identical to the clusters studied here. In order to calculate the relaxation time, a value of $\gamma = 0.02$ was assumed for the Coulomb logarithm (Giersz & Heggie 1996).

We obtain a fairly good agreement with our prediction since the half-mass times scale only slightly steeper than with $t_{rh}^{3/4}$. The slight difference may be due to the core-collapse of the clusters. For the multi-mass clusters core-collapse happens before half-mass is reached and it happens earlier for smaller clusters (cf. Fig. 8), so low-N clusters spend a longer time in the higher mass-loss phases and dissolve quicker. This steepens the scaling of the half-mass times.

The largest single-mass cluster studied dissolves in about 3.5 half-mass relaxation times. If the lifetimes of single-mass clusters continue to scale with $t_{rh}^{3/4}$, they would fall below one relaxation time for clusters containing more than $N = 2.5\ 10^6$ stars, which seems to be rather unlikely. Several reasons could cause a change in the scaling before

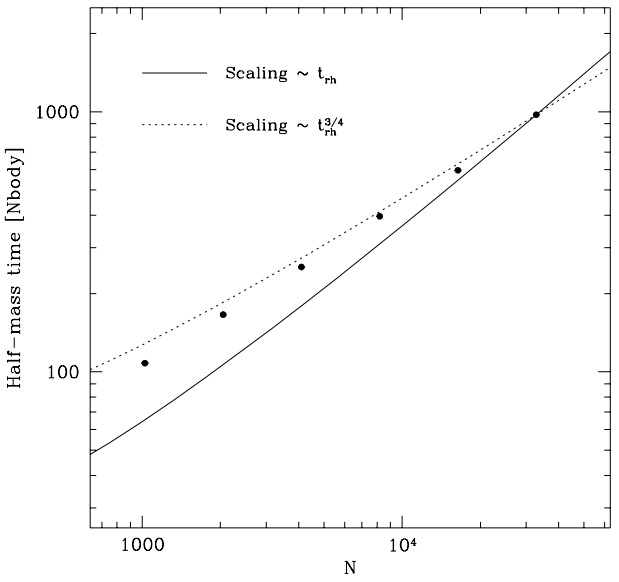

Figure 13. Comparison of the predicted $t_{rh}^{3/4}$ scaling with the dissolution times of multi-mass clusters from the Collaborative Experiment. Like in the case of single-mass clusters, a $t_{rh}^{3/4}$ scaling law gives a fairly good fit to the half-mass times. Multi-mass clusters show a stronger increase in their half-mass times than single-mass clusters due to their earlier core-collapse.

this point is reached: First, we assume an evolution through equilibrium distributions. This assumption will certainly be violated, since, if $t_{Diss} < t_{rh}$, clusters dissolve before any equilibrium can be established. Second our assumption that the number of potential escapers at $\hat{E} = 0$ is proportional to the number of cluster stars might be violated if escape becomes very efficient. Heggie (2000) constructed a cluster in which the number of cluster stars is a function of $\hat{E}$ and t. Solving eq. 12, he could show that the dissolution time scales with t_{rh} if $N \rightarrow \infty$. However, this scaling is reached only for particle numbers beyond the globular cluster regime.

Summarising, it is not clear whether the lifetimes still scale with $t_{rh}^{3/4}$ if N becomes much larger than 10^6. Their scaling up to this point might however be described by such a scaling law. A similar value is found for the multi-mass clusters of the Collaborative Experiment. The $t_{rh}^{3/4}$ scaling might therefore describe the scaling of the lifetimes for most of the globular cluster regime.

4 CONCLUSIONS

The evolution of three different kinds of clusters was studied. It was found that the lifetime scales with the relaxation time only if potential escapers are immediately removed. Otherwise, the lifetime increases more slowly with the particle number than the relaxation time. The reason for this discrepancy is that for radial cut-off clusters and for clusters in a tidal field, there is a difference in time between the moment when stars are scattered above the energy necessary for escape and the moment when they actually leave the cluster. During this time, potential escapers can be scattered back to energies below the critical one and remain bound. This backscattering of potential escapers causes a deviation from a scaling with the relaxation time.

For clusters limited by a radial cut-off, we expect this deviation to vanish for large enough N, since the time needed for escape increases only slowly with the particle number. Since the relaxation time increases almost linear with N, it becomes very large compared to the escape time and all stars scattered above the critical energy leave the cluster, causing the lifetime to scale with the relaxation time.

Clusters in a steady tidal field show a larger discrepancy than the radial cut-off clusters. This is due to the fact that in a tidal field the escape times depend on the energies of the stars and are large for stars with energies only slightly above the critical one. Hence there are always stars that have escape times comparable to their relaxation times and many of them are scattered back to lower energies before they can escape.

If we utilise the result of Fukushige & Heggie (2000), namely that the escape time drops with the energy difference $E_{Star} - E_{Crit}$ to the second power, we expect that the lifetime scales with $t_{rh}^{3/4}$. Such a dependance gives a good fit to the half-mass times of the single-mass clusters studied here and the multi-mass clusters of the Collaborative Experiment (Heggie et al. 1998).

We expect that there will be a transition for very large N beyond which the lifetime scales with the relaxation time. This transition might only play a role for the very largest globular clusters. Other processes, like for example the initial evolution until an equilibrium distribution of potential escapers is established and the core-collapse of the clusters influence the scaling of the lifetimes as well.

Since the lifetimes increase more slowly with the number of cluster stars than the relaxation time, globular clusters will have shorter lifetimes than expected hitherto. More globular clusters might have been destroyed since the time of their formation and the remaining ones have suffered more from dynamical evolution.

Acknowledgements

I thank Douglas Heggie for many valuable comments and suggestions related to this work. I'm also grateful to Toshio Fukushige for the idea to Figure 3, Rainer Spurzem for his help with the NBODY6++ code, and an anonymous referee for his suggestions which improved the presentation of the paper. It is a pleasure to acknowledge the support of the European Commission through TMR grant number ERB FMGE CT950051 (the TRACS Programme at EPCC). The parallel calculations were performed on the CRAY T3E's of HLRZ Jülich and HLRS Stuttgart. H.B. is supported by PPARC under grant 1998/00044.

REFERENCES

Aarseth S., 1999, PASP 111, 1333
Ambartsumian V. A., 1938, Ann. Leningrad State Univ. 22, 19
Chandrasekhar S., 1942, Principles of Stellar Dynamics, Univ. of Chicago Press
Chernoff D.F., Weinberg M.D., 1990, ApJ 351, 121
Fukushige T., Heggie D.C., 1995, MNRAS 276, 206
Fukushige T., Heggie D.C., 2000, MNRAS 318, 753

Giersz M., Heggie D.C., 1994, MNRAS 268, 257
Giersz M., Heggie D.C., 1996, MNRAS 279, 1037
Heggie D.C., 2000, in *Proceedings of the NATO ASI workshop The Restless Universe*, CeMDA preprint
Heggie D.C., Giersz M., Spurzem R., Takahashi K., 1998, in *Highlights of Astronomy*, Vol. 11B, Ed. J. Andersen, D. Reidel Publ. Comp. Dordrecht, p. 591
Hénon M., 1960, Ann. Astrophys. 23, 668
Hénon M., 1969, A&A 2, 151
Johnstone D., 1993, AJ 105, 155
King I., 1959, AJ 64, 351
Makino J., Aarseth S.J., 1992, PASJ, 44, 141
Ostriker J.P., Spitzer L., Chevalier R.A., 1972, ApJ 176, L51
Spitzer L. Jr., 1940, MNRAS 100, 396
Spitzer L. Jr., 1987, Dynamical Evolution of Globular Clusters, Princeton University Press, Princeton
Spurzem R., 1999, in Riffert H., Werner K. (eds), Computational Astrophysics, The Journal of Computational and Applied Mathematics (JCAM) 109, Elsevier Press, Amsterdam, p. 407
Spurzem R., Baumgardt H., 2000, MNRAS submitted
Takahashi K., Portegies Zwart, S., 2000, ApJ 535, 759
Weinberg M.D., 1994a, AJ 108, 1403
Weinberg M.D., 1994b, AJ 108, 1414
Wielen R., 1988, in *The Harlow Shapley Symposium on Globular Cluster Systems in Galaxies*, Eds. J.E. Grindlay and A.G.D. Philip, D. Reidel Publ. Comp. Dordrecht, p. 393

This paper has been produced using the Blackwell Scientific Publications LaTeX style file.